Pharm Res (2013) 30:412–423
DOI 10.1007/s11095-012-0883-5

RESEARCH PAPER

PEGylated Multi-Walled Carbon Nanotubes for Encapsulation and Sustained Release of Oxaliplatin

Linlin Wu • Changjun Man • Hong Wang • Xiaohe Lu • Qinghai Ma • Yu Cai • Wanshan Ma

Received: 30 May 2012 / Accepted: 5 September 2012 / Published online: 20 September 2012

ABSTRACT

Purpose To develop PEGylated multi-walled carbon nanotubes as a sustained release drug delivery system.

Methods Oxaliplatin was incorporated into inner cavity of PEGylated multi-walled carbon nanotubes (MWCNT-PEG) using nano-extraction. Oxaliplatin release rates from MWCNT-PEG-Oxaliplatin were investigated using dialysis tubing. Cytotoxicity of oxaliplatin, MWCNT-Oxaliplatin and MWCNT-PEG-Oxaliplatin were evaluated in HT29 cell by MTT assay, Pt-DNA adducts formation, γ-H2AX formation and cell apoptosis assay.

Results Loading of oxaliplatin into MWCNT-PEG was ~43.6%. Sustained release occurred to MWCNT-PEG-Oxaliplatin, with only 34% of oxaliplatin released into medium within 6 h. In MTT assay, MWCNT-PEG-Oxaliplatin showed slightly decreased cytotoxic effect when cell viability was assessed at 12 and 24 h. A drastic increase of cytotoxicity was found when cell viability was assessed at 48 and 96 h. Pt-DNA adducts formation, γ-H2AX formation and cell apoptosis assay results showed the same trend as the MTT assay, suggesting sustained-release for MWCNT-Oxaliplatin and MWCNT-PEG-Oxaliplatin formulations.

Conclusions PEGylated multi-walled carbon nanotubes can be used as sustained release drug delivery system, thus remarkably improving cytotoxicity of oxaliplatin on HT-29 cells.

KEY WORDS carbon nanotube · cytotoxicity · HT29 cell line · oxaliplatin · PEGylation

ABBREVATIONS

AAS	atomic absorption spectroscopy
CNTs	carbon nanotubes
DSBs	DNA double-strand breaks
MWCNT	multi-walled carbon nanotubes
MWCNT-PEG	PEGylated multi-walled carbon nanotubes
Pt	platinum
TEM	transmission electron microscopy
TGA	thermal gravimetric analysis

INTRODUCTION

Oxaliplatin, a third-generation platinum analog of the 1,2-diaminocyclohexane families, induces DNA cross-link leading to DNA double-strand breaks (DSBs) (1). Although it shares various mechanistic properties with the parent platinum drug, cisplatin, oxaliplatin has a broad spectrum of antineoplastic activity including colon, ovarian and lung cancer. It has

L. Wu and C. Man contributed equally to this paper.

L. Wu • Q. Ma • W. Ma (✉)
Department of Laboratory Medicine
Shandong Provincial Qianfoshan Hospital & Shandong University
16766 Jingshi Road
Jinan, People's Republic of China, 250014
e-mail: wanshan.ma@gmail.com

C. Man
Department of Clinical Laboratory
Jining Hospital of Infectious Diseases
Jiumiguzui Northern Suburb of Jining
Jining, People's Republic of China, 272031

H. Wang
Shandong Provincial Qianfoshan Hospital
16766 Jingshi Rd., Jinan, People's Republic of China, 250014

X. Lu
Shandong Academy of Medical Sciences
Shandong Provincial Qianfoshan Hospital
16766 Jingshi Rd., Jinan, People's Republic of China, 250014

Y. Cai
School of Pharmacy, Jinan University
601 W Huangpu Rd., Guangzhou, People's Republic of China, 510632

demonstrated a lack of cross-resistance with other platinum compounds and been widely applied in chemotherapy (2). However, like the other chemotherapeutic platinum agents, oxaliplatin also suffers the development of tumor cell resistance, which might come from the reduced cellular drug accumulation, inactivation by conjugation with glutathione, enhanced tolerance or increased excision-repair of platinun-DNA adducts (2–4). Furthermore, its treatment is also associated with side effects (neutropenia, ototoxicity, hyperkalemia, etc.) (5–7). To overcome these limitations, various carriers for oxaliplatin, including polymer micelles (8), liposomes (9,10), and microspheres (11), have been developed and investigated.

Since carbon nanotubes (CNTs) were discovered by Iijima in 1991 (12), the studies of CNTs have progressed rapidly in many fields, and currently they are also used as carriers for drug delivery in nanotechnology (13). Their needle-like structure with high length-to-diameter ratio is advantageous to pass through cell membranes (14), moreover, their huge surface area and inner hollow space are very good scaffold for the attachment of drug molecules (15). The stability of CNTs allows various chemical modifications on their tips and surface, improving their biocompatibility and binding to the bioactive agents as well (16,17). So far, a lot of studies of CNTs as drug delivery system have been reported, including the entrapment into inner cavity by adsorption and attachment on the external surface by chemical binding. Ajima and his colleagues (18) have used oxidised single-walled carbon nanohorns (SWCNHs) to entrap cisplatin and investigated its effect on the growth of human lung cancer cells. Feazell and his colleagues (19) have developed a longboat structure tethering single-walled carbon nanotubes (SWCNTs) with *c*, *c*,*t*-[Pt(NH_3)$_2$$Cl_2$(OEt)($O_2CCH_2CH_2CO_2H$)] to deliver the platinum-based drug into cells. There are still great concerns of their toxicity and biocompatibility in the application, since pristine CNTs are toxic to cells and adequate functionalisation is needed to eliminate or mitigate this kind of harm (20,21). In previous study, we explored the use of multi-walled carbon nanotubes (MWCNTs) as a suitable drug carrier with good biocompatibility, excellent loading efficiency and capability to take drug into cancer cells. Hence we modified multi-walled carbon nanotubes (MWCNTs) with PEG 600 and encapsulated oxaliplatin into the PEGylated MWCNTs (MWCNT-PEG), expecting to attain sustained release of entrapped oxaliplatin and the improvement of cytotoxicity to tumor cells.

MATERIALS AND METHODS

Materials

Oxaliplatin (Fig. 1) was purchased from Singapore Merlin Standard Chemicals Pte. Ltd. MWCNTs were purchased from Nanjing XFNANO Materials Tech Co., Ltd. PEG 600 was purchased from Sigma Aldrich. All other chemicals were purchased from Shanghai Yuanxi International Trade Co., Ltd. TEM was carried out using JEM 2010F HRTEM (JEOL). TGA was performed on a Perkin-Elmer Instruments, Pyris Diamond TG/DTA Thermogravimetric/Differential Thermal Analyzer, with a heating rate of 10°C/min in air. AAS was measured using Perkin Elmer PinAAcle 900 Atomic Absorption Spectrometer.

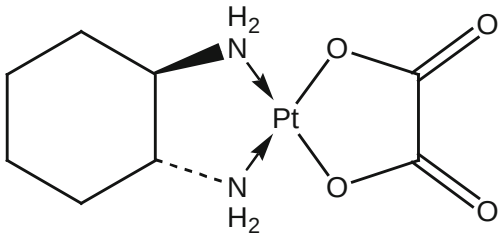

Fig. 1 Chemical structure of oxaliplatin.

Synthesis of MWCNT-PEG

In the first step, purified MWCNTs (100 mg) were immersed in a mixture of 98% H_2SO_4 and 65% HNO_3 (3:1, *v*/*v*), followed by ultrasonication for 5 h. After that, the MWCNTs acidic mixture was diluted with water and centrifuged for 4~6 times to decrease the acid content until pH 5~6 was reached. The powder form of oxidised MWCNTs (MWCNT-COOH) was dried in vacuum.

The second step was to functionalise MWCNT-COOH with PEG 600. MWCNT-COOH was dispersed in 20 ml of oxalyl chloride under ultrasonication. The mixture was stirred at 60°C for 6 h, and subsequently excess oxalyl chloride was evaporated under vacuum. The dry powder was dispersed in 20 ml anhydrous DMF and reacted with PEG 600 (1 g, MW=600). After stirring at 100°C for 5 days, the mixture was filtered through a 0.2 μm membrane and rinsed with DMF, ethanol, and deionized water. The product PEGylated MWCNTs (MWCNT-PEG) were collected from the filter membrane and dried under vacuum (90 mg) (Scheme 1). To test their solubility in water, a certain amount of MWCNTs with or without functionalisation were dispersed in water of specific volume under 30 min ultrasonication, and the dispersion of MWCNTs was then centrifugated at 1,000 rcf for 5 min; if there was no precipitation following the centrifugation, MWCNTs were considered to be soluble at such concentration, i.e. the solubility in water.

Oxaliplatin Incorporation into MWCNT-COOH and MWCNT-PEG

Oxaliplatin was incorporated into the inner cavity of MWCNTs using nano-extraction method. MWCNT-

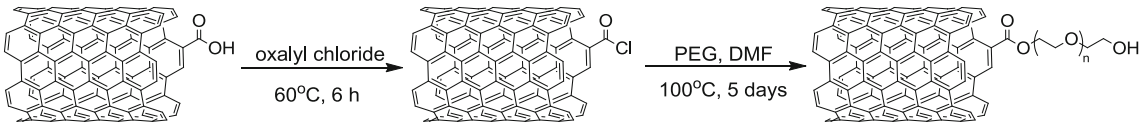

Scheme I Synthesis of MWCNT-PEG.

COOH (40 mg) or MWCNT-PEG (40 mg) was dispersed in 20 ml ethanol under ultrasonication to give a suspension. Oxaliplatin (100 mg) was added to the suspension, and stirred at room temperature for 3 days. After that, the mixture was filtered through a 0.2 μm membrane and rinsed with ethanol and deionized water to eliminate unincorporated Oxaliplatin. The product MWCNT-Oxaliplatin and MWCNT-PEG-Oxaliplatin were collected from the filter membrane and dried under vacuum (77 mg MWCNT-Oxaliplatin; 68 mg MWCNT-PEG-Oxaliplatin). The obtained powders were observed using transmission electron microscope (TEM).

Oxaliplatin Release from MWCNT-Oxaliplatin and MWCNT-PEG-Oxaliplatin

The rate of oxaliplatin release from MWCNT-Oxaliplatin and MWCNT-PEG-Oxaliplatin was investigated using dialysis tubing method. MWCNT-Oxaliplatin or MWCNT-PEG-Oxaliplatin (containing 3 mg of oxaliplatin) was first dispersed in 2 ml PBS and placed inside a cellulose dialysis tube with 10 kDa pore size, which was subsequently immersed in 498 ml PBS under stirring. The oxaliplatin was released from inner cavity of MWCNT-COOH or MWCNT-PEG and diffused out of the dialysis tube, therefore 2 ml samples of the release medium were periodically withdrawn and also replaced with fresh PBS. The amounts of Pt in these samples were measured using atomic absorption spectrometer (AAS).

Cell Culture and MTT Assay

The human colon adenocarcinoma HT29 cells (HTB-38, ATCC) were routinely maintained in McCoy's 5a Medium (Sigma), which was supplemented with 10% fetal bovine serum, 0.37% sodium bicarbonate, L-glutamine (0.03%, *w/v*), 100 U/ml penicillin and 100 μg/ml streptomycin. Cultures were maintained at 37°C and 5% CO_2 in a humidified incubator. To evaluate the cytotoxicity of MWCNT, MWCNT-PEG, oxaliplatin, MWCNT-Oxaliplatin and MWCNT-PEG-Oxaliplatin, 100 μl (1×10^4 cells) of HT29 cells were seeded in 96-well plate to obtain exponential growth. After a 24 h incubation, cells were then exposed to different concentrations of formulations. At the end of indicated incubation period, growth inhibition was determined by MTT assay as previously described (22). For each formulation, the results are expressed as the relative percent absorbance compared with controls without treatment.

Measurement of Pt-DNA Asdducts

Pt-DNA adducts were measured as described by Walker *et al.* (23,24). HT29 cells grown to 70–80% confluence on 10-cm tissue culture dishes were treated with 5 μM of oxaliplatin, MWCNT-Oxaliplatin or MWCNT-PEG-Oxaliplatin. After 12 or 96 h of incubation, the cells were washed twice with cold PBS and DNA samples were extracted using the Flexigene Kit (Qiagen) following the manufacturer's instructions. The samples were stored at −20°C and sonicated just before analysis. Platinum (Pt) content was determined by AAS using Perkin Elmer PinAAcle 900 Atomic Absorption Spectrometer as previously reported (25). And the Pt concentrations in the samples were calculated from a standard curve (0.5–30 ng Pt per ml). The DNA concentration was estimated by measuring absorbance at 260 nm. Results (pg Pt per μg DNA) are expressed as the mean ± SD of six independent experiments.

Cell Apoptosis Analysis

To evaluate the cell apoptosis induced by oxaliplatin, MWCNT-Oxaliplatin or MWCNT-PEG-Oxaliplatin, HT29 cells were plated at 5×10^4 cells /well in a 96-well plate. After 24 h of incubation, the cells were treated with 5 μM of each formulations and the incubation was continued for another 12, 24, 48 or 96 h. At the end of each treatment, samples were harvested and analyzed for histone-associated DNA fragments using a Cell Death ELISA^{PLUS} Kit (Roche Molecular Biochemicals) according to the manufacturer's instructions. The test is based on a quantitative sandwich-enzyme-immunoassay principle, using mouse monoclonal antibodies directed against DNA and histones, respectively. This allows the specific detection and quantitation of mono- and oligonucleosomes that are released into the cytoplasm of cells that die from apoptosis. Their enrichment in the cytoplasm is calculated as absorbance of sample cells/absorbance of control cells. The enrichment factor was used as a measure of apoptosis and is shown as mean ± SD.

Western Blotting

HT29 cells that were treated with 5 μM of oxaliplatin, MWCNT-Oxaliplatin or MWCNT-PEG-Oxaliplatin were incubated for another 12 h or 96 h. Total cell lysates were prepared by homogenizing the cell pellets in lysis buffer (Cell Signaling Technology, USA) containing freshly added protease inhibitor cocktail (Roche Diagnostics, Germany).

Proteins in whole cell lysates were electrophoresed on a SDS-polyacrylamide gel, and transferred to a nitrocellulose membrane. Nonspecific binding was blocked with 5% nonfat milk for 1 h at room temperature. After immunoblotting with the first specific antibodie (γH2AX, Santa Cruz Biotechnology, Inc), membranes were washed three times with TBST and incubated with horseradish peroxidase-conjugated secondary antibodie (Santa Cruz Biotechnology, Inc) for 1 h. Membranes were then visualized by enhanced chemiluminescence [SuperSignal West Femto (Pierce, USA)]. To make sure equal amounts of sample protein were applied for electrophoresis and immunoblotting, β-actin (Santa Cruz Biotechnology, Inc) was used as an internal control.

Statistical Analysis

Differences between the mean values of two subgroups were evaluated using Student's t-test. Differences between the mean values of three subgroups were compared by one-way analysis of variance (ANOVA). p values$\leq$0.05 were considered statistically significant.

RESULTS AND DISCUSSIONS

Characterisation of MWCNT-Oxaliplatin and MWCNT-PEG-Oxaliplatin

The chemistry of CNTs has been developed to introduce various functional groups to the surface and extremetries of CNTs with the purpose of changing its physicochemical property and binding with drug molecules (16). Various hydrophilic molecules were attached onto CNTs to facilitate their suspendability in water or organic solvents and to decrease their toxicity, which is a great consideration to exploit CNTs as vehicle for drug delivery. Therefore, in our case, MWCNTs were functionalised with PEG to improve their hydrophilicity and it was found that the solubility of different MWCNTs in water increased with their functionalisation degree. The purified MWCNTs without functionalisation had very poor solubility of 0.026 mg/ml in water, while the solubility of oxidised MWCNTs increased to 1.3 mg/ml due to the carboxylic groups. And this solubility further reached 4.5 mg/ml after the functionalisation with PEG. In comparison, the excellent solubility of MWCNT-PEG in water was highly advantageous to be a vehicle.

The MWCNT-COOH and MWCNT-PEG were observed under TEM to identify morphological characterization. Their length ranged from a few hundred nanometers to a few micrometers, and their outer diameter was 40–50 nm with approximately 15 nm thickness of multi-walls (Fig. 2). Their images showed that both of MWCNT-COOH and MWCNT-PEG had clean multiwall and inner cavity. While the outside boundary of MWCNT-COOH was bare (Fig. 2a), the outside the MWCNT-PEG was a grayish coating layer (Fig. 2b), which was possibly due to the attachment of PEG on the surface of MWCNT-PEG.

To confirm the PEGylation of MWCNT-PEG, TGA was used to analyse the loading of PEG in MWCNT-PEG based on the comparison of metal residue after high temperature heating. These trace metal was from metal catalyst during manufacturing, and it was stable at high temperature, which could combust the MWCNTs, PEG, and functional groups in metallic compounds. Hereby the metal content was considered as a constant parameter of MWCNTs. Figure 3 showed the TGA graphs and the derivative curves of MWCNT-COOH and MWCNT-PEG. The combustion temperature of MWCNT-COOH in air was around 620°C (Fig. 3a), whereas it decreased about 100°C after conjugation with PEG (Fig. 3b). The decomposition temperature of PEG portion in MWCNT-PEG was around 380°C, This difference therefore separated the peaks of MWCNTs and PEG clearly in the derivative curve of MWCNT-PEG. The weight percentage of metal residue was respectively 7.0% for MWCNT-COOH (Fig. 3a) and 5.8% for MWCNT-PEG (Fig. 3b), therefore the loading of PEG in MWCNT-PEG was estimated to be 17%, and the degree of functionality in MWCNT-PEG was 0.28 mmol of PEG for each 1 g of MWCNT-PEG.

The MWCNT-Oxaliplatin and MWCNT-PEG-Oxaliplatin, which were prepared using nano-extraction method (26), were observed under TEM, and the loading of oxaliplatin in them was also estimated using TGA. In their TEM images, the multi-walls and inner cavity of MWCNT-Oxaliplatin and MWCNT-PEG-Oxaliplatin were not as clean as that of MWCNT-COOH and MWCNT-PEG, and indeed plenty of "dirty" particulates located along their inner cavities and were also randomly distributed within their multi-walls. To identify the property of these particulates, EDX was performed on them to analyse their elements. The result showed that the regions comprising dense particulates had strong Pt signal, while Pt signal was very weak in other regions with few particulates, thus suggesting that the particulates consisted of oxaliplatin molecules, which stuck to the inner cavity and external surface of MWCNTs (Fig. 4). It was also found that the "dirty" particulates on the multi-walls of MWCNT-PEG-Oxaliplatin were thicker than that of MWCNT-Oxaliplatin, although washing procedure were performed on both of them. We postulated that the PEG branches on the surface of MWCNT-PEG entrapped oxaliplatin molecules, which were able to escape from the washing procedure due to their strong affinity, whereas the external surface of MWCNT-COOH was relatively smooth and had only weak affinity with oxaliplatin molecules, thus allowing the washing agent to remove excessive drug molecules.

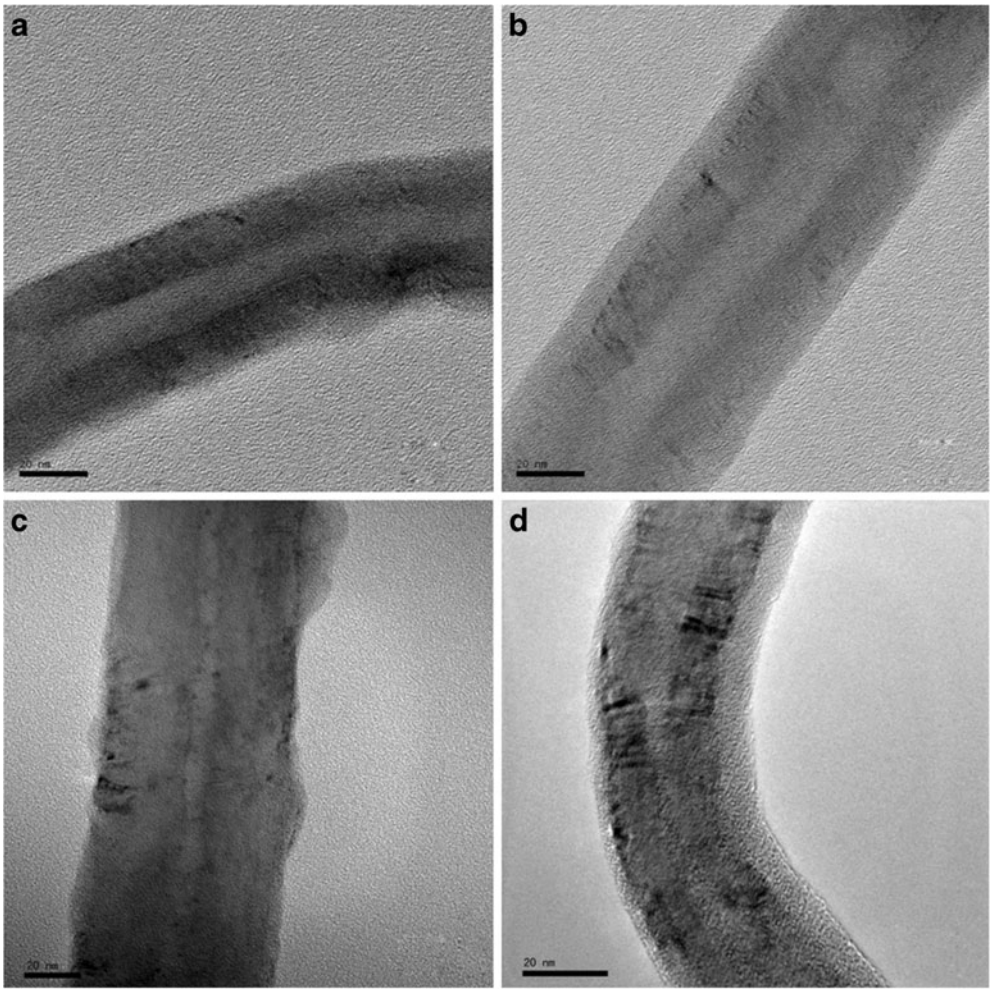

Fig. 2 TEM images of (**a**) MWCNT-COOH; (**b**) MWCNT-PEG; (**c**) MWCNT-Oxaliplatin and (**d**) MWCNT-PEG-Oxaliplatin.

The loading of oxaliplatin in MWCNT-Oxaliplatin and MWCNT-PEG-Oxaliplatin was analysed using TGA on the basis of metal residue. The derivative curves of MWCNT-Oxaliplatin (Fig. 3c) and MWCNT-PEG-Oxaliplatin (Fig. 3d) showed their combustion process. The first weight loss occurred at about 300°C corresponding to oxaliplatin degradation, in which elements of C, H, O, N combusted leaving behind only platinum residue. When the temperature increased to about 380°C, another weight loss presented in only MWCNT-PEG-Oxaliplatin (Fig. 3d), thus corresponding to the decomposition of PEG, while the combustion temperature of MWCNTs portion was about 510°C for both of MWCNT-Oxaliplatin and MWCNT-PEG-Oxaliplatin. The metal residue after TGA combustion was respectively 28.7% for MWCNT-Oxaliplatin (Fig. 3c) and 24.7% for MWCNT-PEG-Oxaliplatin (Fig. 3d) by weight. Taking into account that MWCNT-COOH and MWCNT-PEG also contained 7.0% and 5.8% of metal residue, the loading of oxaliplatin was estimated to be 51.5% for MWCNT-Oxaliplatin and 43.6% for MWCNT-PEG-Oxaliplatin, respectively. We assumed that PEG branches at the extermetries of MWCNT-PEG might obstruct oxaliplatin molecules from entering its inner cavity, and the MWCNT weight also increased by about 20% on account of PEGylation, therefore less oxaliplatin was entrapped in MWCNT-PEG than that in MWCNT-COOH.

Oxaliplatin Release from MWCNT-Oxaliplatin and MWCNT-PEG-Oxaliplatin

The hydrophilic oxaliplatin incorporated inside inner cavity could be easily displaced by water molecules and move out of MWCNTs, since its affinity with hydrophobic inner surface of MWCNTs was weaker than that with water molecules in release medium. Similar study of cisplatin release has been reported by other groups (27). In our case, the release of oxaliplatin from MWCNT-Oxaliplatin was very quick within the 3 h, and even 50% of incorporated drug was detected in the medium within 6 h, whereas its release reached plateau after 24 h, and finally 89% of drug was recovered within 5 days (Fig. 5). Ajima and his colleagues reported the slow release of cisplatin from SWCNHs with the hole size of 0.5–1.5 nm diameter (18), although cisplaitn was also hydrophilic and had strong affinity

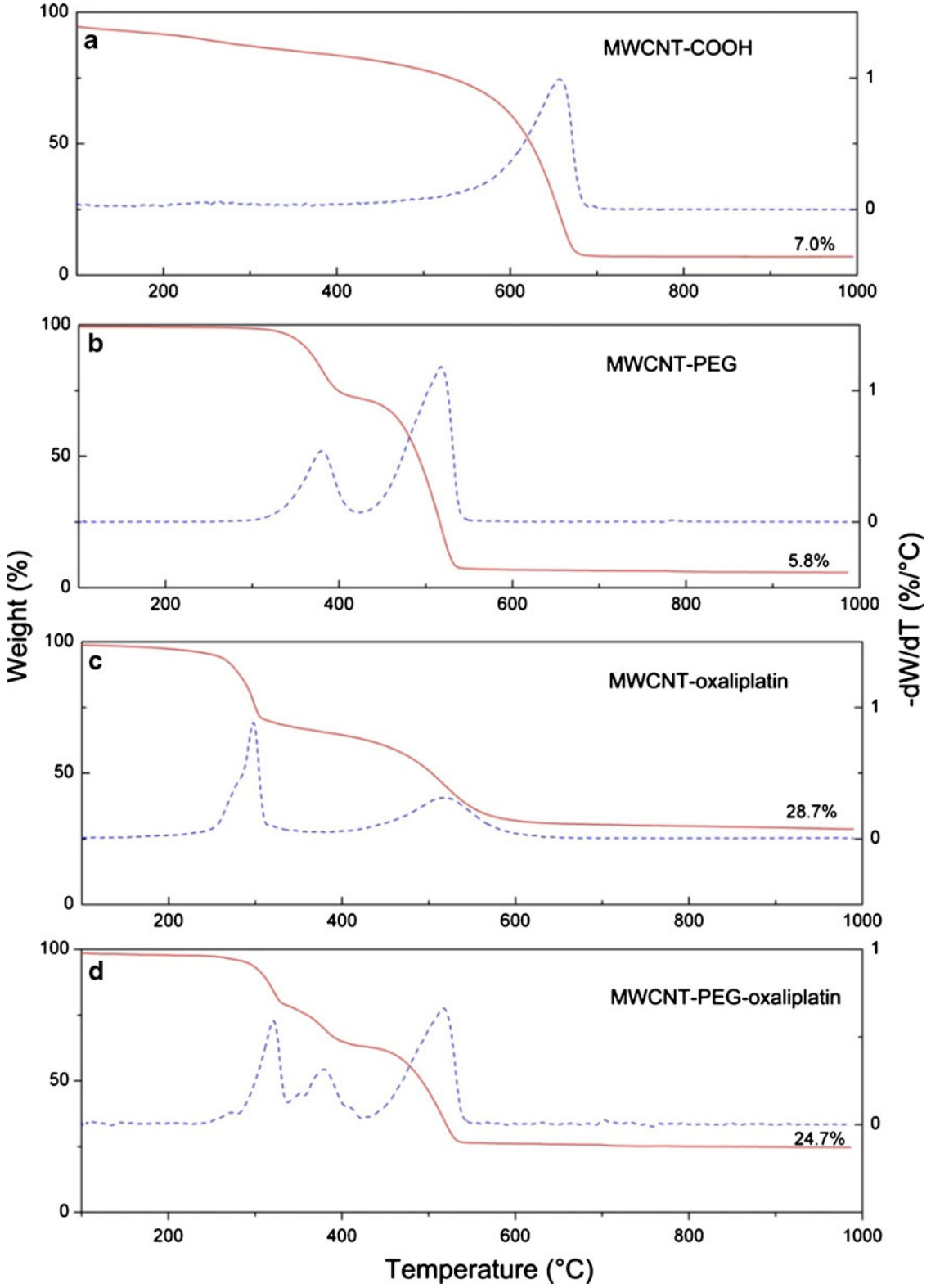

Fig. 3 TGA graphs and derivative curves of (**a**) MWCNT-COOH; (**b**) MWCNT-PEG; (**c**) MWCNT-Oxaliplatin; (**d**) MWCNT-PEG-Oxaliplatin. The TGA graphs are labeled with the wt.% of metal residue after ramping the sample to 1000°C at a rate of 10°C/min in air.

with water. Taking account of the cone-shape structure of SWCNHs and their thin cavity size relative to cisplatin and water molecules, it is possible that the release of incorporated molecules was also dependent on hole size,

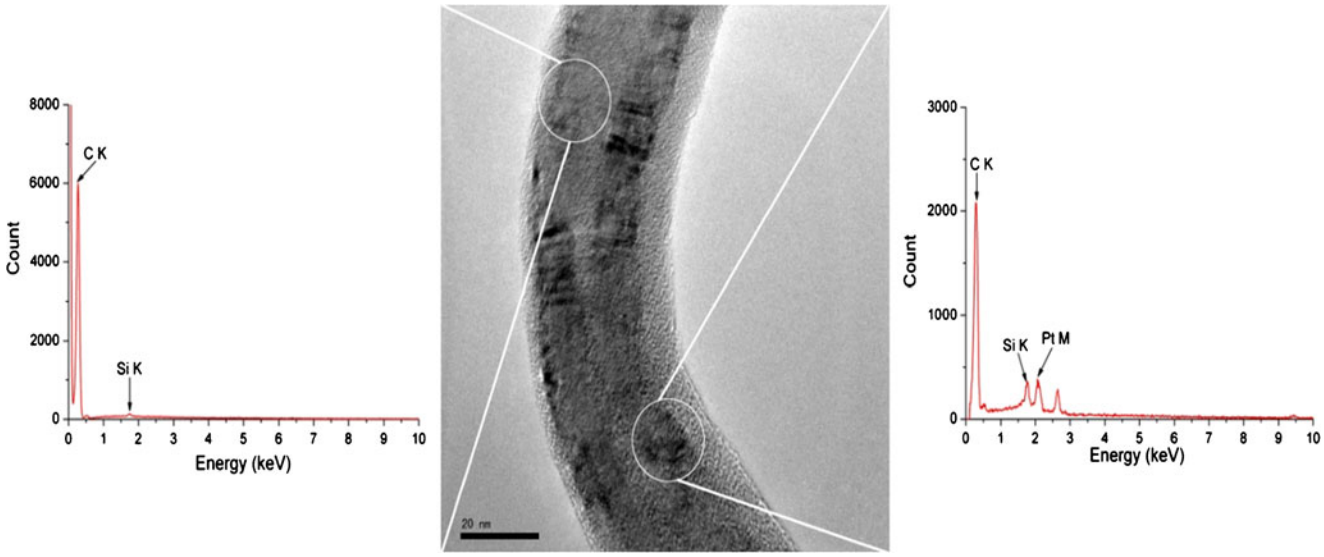

Fig. 4 EDX spectrum from different location of MWCNTs. The left EDX spectrum is from position containing no black particulates, showing C 93.36% and Si 0.71% by weight, but no Pt signal was detected. The right EDX spectrum is from position containing abundant black particulates, showing C 71.22%, Si 2.33% and Pt 13.64% by weight.

which was a crucial factor in migration, therefore water molecules together with oxaliplatin were able to smoothly flow through the MWCNTs with large hole size of about 10 nm diamter.

On the other hand, slower release of Oxaliplatin occurred to MWCNT-PEG-Oxaliplatin. Only 34% of Oxaliplatin was found in the medium after 6 h, and its plot showed a mild ramp between 18 h and 120 h (Fig. 5). This was in agreement with the study of plug effect caused by functional groups at hole edges (28), which concluded that the functional groups at the hole edges of carbon nanohorns could plug the holes, leading to the small quantity of cisplatin release at slow rate. In our study, the long-chain PEG at the hole edges of MWCNTs also blocked a part of the holes and reduced their effective diameter, thus causing an obstacle to movement of oxaliplatin molecules, although

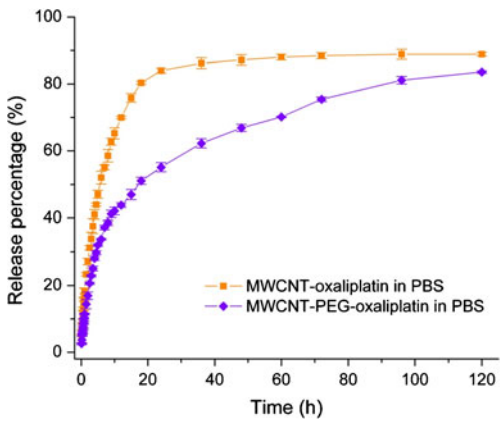

Fig. 5 Release plot of oxaliplatin from MWCNT and MWCNT-PEG in PBS.

MWCNTs had large original diameter of about 10 nm. This result suggested that MWCNT-PEG-Oxaliplatin had better effect of sustained release to prevent drug dissipation before reaching the tumor.

Cytotoxicity Evaluation of Oxaliplatin, MWCNT-Oxaliplatin and MWCNT-PEG-Oxaliplatin on HT29 Human Colon Adenocarcinoma Cells

The cytotoxicity of Oxaliplatin, MWCNT-Oxaliplatin and MWCNT-PEG-Oxaliplatin on HT29 human colon adenocarcinoma cells were firstly evaluated with a MTT method. In the MTT assay, mitochondrial dehydrogenases cleave the tetrazolium ring and reduce MTT to insoluble dark blue formazan crystals. Only active mitochondria contain these enzymes and, therefore, the reaction only occurs in viable cells. Absorbance, directly proportional to cell viability, was determined at 550 nm in a Bio-rad microplate reader. The absorbance values were normalized by the controls and expressed as percent viability. There were reports suggested that the MTT method is not reliable for finding out the cytotoxity of CNT based materials, as the MTT formazan crystals formed in the MTT reaction are lumped. As a consequence, false results may show a strong cytotoxic effect (29–31). However, there are still studies that use this method to assay the toxicity of MWCNT (27,32). In our experiment, the cell viability of HT29 remained at high percentage after treatment with 1–8 μM of MWCNT or MWCNT-PEG (Fig. 6). This result suggested that MWCNT did not interfere with MTT assay in our case. We deduce the variation from different reports to the difference in MTT concentration used in the assay (the lower

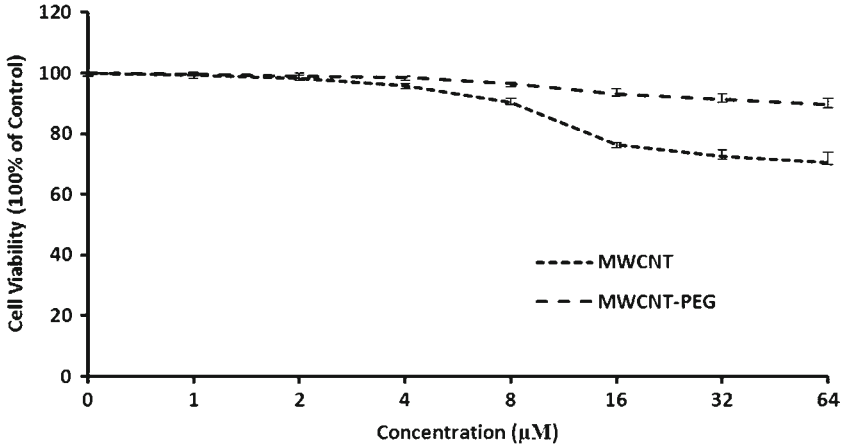

Fig. 6 Dose-dependent cytotoxicity curves of MWCNT and MWCNT-PEG in HT29 human colon adenocarcinoma cells after a 48 h treatment. The concentrations of MWCNT and MWCNT-PEG were nominalized by their corresponding concentrations in MWCNT-Oxaliplatin and MWCNT-PEG-Oxaliplatin and were presented in the molar concentration of Oxaliplatin. Data represent the mean ± SD of three independent experiments.

in MTT concentration, the less precipitation be formed), time intervals between MTT addition and detection (the shorter in the time interval, the less interference be observed), and even the quality of MWCNT purchased from different manufactures. When concentrations of MWCNTs and MWCNT-PEG gradually increased to a higher level (64 μM), the pristine MWCNTs group had a rapid decrease of viability to about 70%, whereas the MWCNT-PEG was still maintained above 90% (Fig. 6). This result suggested that pristine MWCNTs would still lead to cell death at high concentrations, while its cytotoxicity could be overcome by functionalisation with PEG. It is possible that the surface of MWCNTs was enshrouded by PEG molecules after PEGylation, therefore MWCNT-PEG improved its solubility and biocompatibility in comparison to pristine MWCNTs. Furthermore, the length MWCNT was shortened in the process of oxidation, thus helping reduce its cytotoxicity as well (21).

When oxaliplatin was loaded onto MWCNT-COOH or MWCNT-PEG, the formulations yielded different cytotoxicity at different treatment time points. Compared with the free oxaliplatin, MWCNT-Oxaliplatin and MWCNT-PEG-Oxaliplatin showed a slightly decreased cytotoxic effect when the cell viability was assessed at 12 and 24 h (Fig. 7a and b). The decrease might originate from the retarded release of oxaliplatin from MWCNT-Oxaliplatin or MWCNT-PEG-Oxaliplatin. The *in vitro* release test showed that most of the incorporated oxaliplatin was diffused into medium in a relatively short time. While only 50% of oxaliplatin was released from MWCNT-PEG-Oxaliplatin, more than 80% the oxaliplatin was released from MWCNT-Oxaliplatin within 20 h (Fig. 5). This explains why MWCNT-PEG-Oxaliplatin showed a more reduced cytotoxicity than MWCNT-Oxaliplatin (Fig. 7a and b). In comparison, a drastic enhancement of cytotoxic effect occurred in MWCNT-Oxaliplatin and MWCNT-PEG-Oxaliplatin when the cell viability was assessed at 48 and 96 h (Fig. 7c and d). This could be due to the increased cellular uptake of oxaliplatin with the help of MWCNT-COOH or MWCNT-PEG, which could penetrate cell membrane and carry the incorporated oxaliplatin into cells. In addition, it was found that MWCNT-PEG-Oxaliplatin had a slower release of oxaliplatin, avoiding the outflow of oxaliplatin before entering cells, and the internalised MWCNT-PEG-Oxaliplatin could keep releasing oxaliplatin even after 100 h exposure (Fig. 5). Therefore, it could have excellent follow-up release after normal exposure.

Previous studies have indicated that DNA is the primary cellular target of platinum and the level of platinum-DNA adducts is an important marker for clinical biological effect of platinum-based chemotherapy (33,34). The decrease in Pt-DNA adducts that resulted from an increase in DNA repair is clearly an important effector of resistance to platinum-based DNA-damaging agents (35). In our experiment, a 12 h treatment of HT29 cells with 5 μM of oxaliplatin, MWCNT-Oxaliplatin or MWCNT-PEG-Oxaliplatin increased the formation of Pt-DNA adducts, with oxaliplatin showing the greatest potential and followed by MWCNT-Oxaliplatin and MWCNT-PEG-Oxaliplatin (Fig. 8). However, when the treatment time extended to 96 h, the activity of the three formulations showed a reverse rank in inducing Pt-DNA adducts formation, with MWCNT-PEG-Oxaliplatin showing the greatest potential. The decrease of platinum-DNA adduct levels in the oxaliplatin and MWCNT-Oxaliplatin treated groups at the time point of 96 h might originate from the proliferation of HT29 cells, which produced more DNA content, leading to a reduced Pt/DNA ratio. While in the MWCNT-PEG-Oxaliplatin treated group, the relatively enhanced cytotoxicity inhibited the cell proliferation and increased cell apoptosis. Therefore, less DNA was produced and the Pt/DNA ratio was higher than the other two groups. The phosphorylated H2AX, designated as γ-H2AX, is another important marker of ionizing radiation or genotoxic agents-induced DSBs (36).Within minutes of the induction of DNA double-strand breaks, histone H2AX becomes phosphorylated in the serine 139 residue at the damage site. The

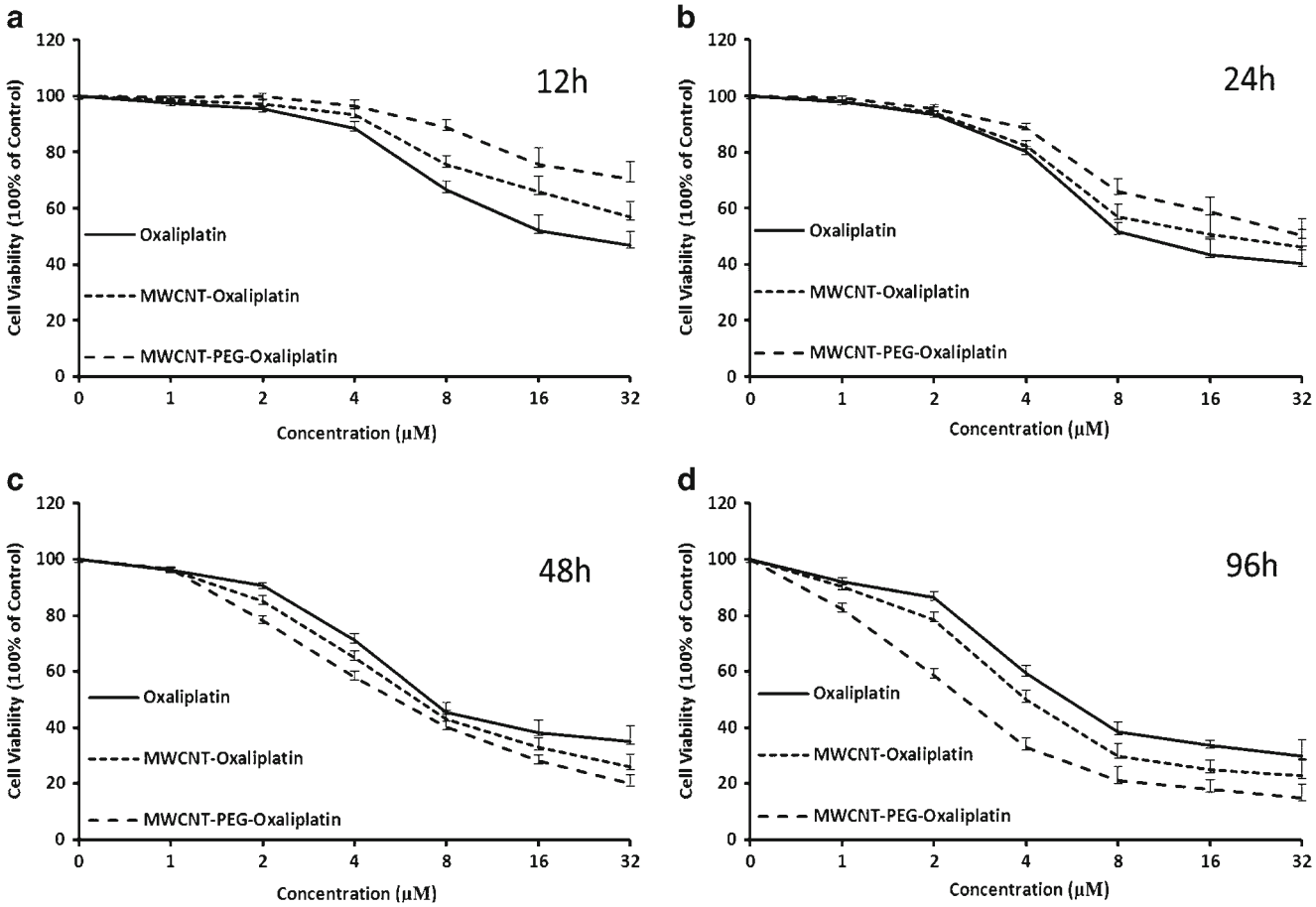

Fig. 7 Dose-dependent cytotoxicity curves of oxaliplatin, MWCNT-Oxaliplatin and MWCNT-PEG-Oxaliplatin in HT29 human colon adenocarcinoma cells after a (**a**) 12, (**b**) 24, (**c**) 48 and (**d**) 96 h treatment. The corresponding concentrations of MWCNT-Oxaliplatin and MWCNT-PEG-Oxaliplatin were calibrated based on their drug loading of 51.5% for MWCNT-Oxaliplatin and 43.6% for MWCNT-PEG-Oxaliplatin. Data represent the mean (±SD) of three independent experiments.

phosphorylation of H2AX at DSBs timely recruits and/or retains DNA repair and checkpoint proteins such as BRCA1, MRN complex, MDC1 and 53 bp1 to sites of DNA damage, activating downstream signal pathways that ultimately resulting in DNA damage repair, cell cycle arrest or apoptosis (37–40). Our results showed that while none of γ-H2AX had been detected in the control group, 5 μM of oxaliplatin, MWCNT-Oxaliplatin and MWCNT-PEG-Oxaliplatin induced the formation of γ-H2AX in HT29 cells after a 12 and 96 h treatment. The efficacy in inducing γ-H2AX formation showed the same trend as they induce the Pt-DNA adducts formation (Fig. 9). That is, with the extension of treatment time, MWCNT-PEG-Oxaliplatin showed more potential. Finally, the oxaliplatin, MWCNT-Oxaliplatin and MWCNT-PEG-Oxaliplatin induced cell apoptosis was evaluated. As shown in Fig. 10, the proportion of apoptosized cells increased with the extension of treatment time for all the three formulations. In accordance with the MTT assay, Pt-DNA adducts formation and γ-H2AX formation results, oxaliplatin showed a higher apoptosis induction activity than MWCNT-Oxaliplatin and MWCNT-PEG-Oxaliplatin when the HT29 cells were treated for 12 or 24 h. But when the treatment time increased to 48 h or 96 h, the induction activity rank reversed, with MWCNT-PEG-Oxaliplatin showing the greatest efficiency. These results, taken together, suggested a sustained-release manner for the MWCNT-Oxaliplatin and MWCNT-PEG-Oxaliplatin formulations.

In clinical cancer chemotherapy, to adopt high dose of drugs for patients so as to achieve maximum treatment efficacy is one of the commonly employed strategies. Nevertheless, administration of high dose anti-cancer agents is accompanied by unbearable side effects. Furthermore, the high administration frequency inevitably reduces the patients' life quality, which in turn disadvantages the patients' recovery. To develop efficient cellular uptake and sustained-release formulations for anti-cancer drugs have come to one of the research focuses. Carbon nanotubes have been used as vehicle for bioactive or drug molecules

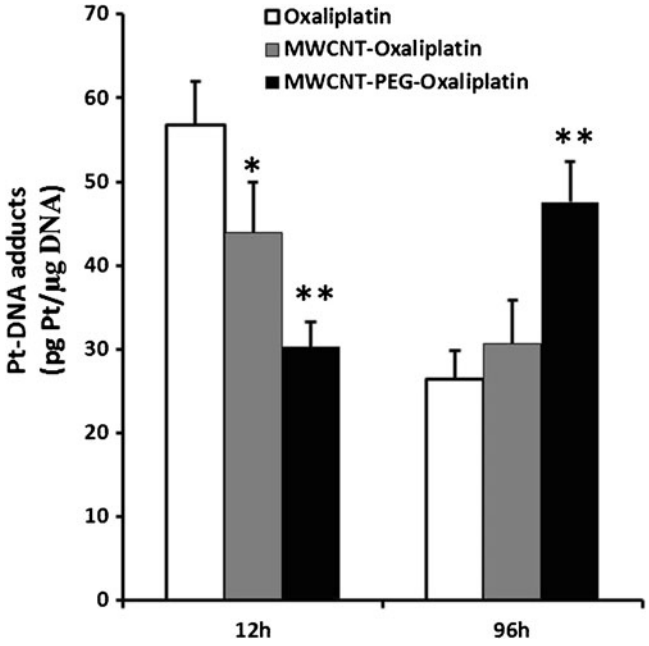

Fig. 8 Effect of oxaliplatin, MWCNT-Oxaliplatin and MWCNT-PEG-Oxaliplatin on Platinum-DNA adduct formation in HT29 human colon adenocarcinoma cells after a 12 and 96 h treatment. Data represent the mean (±SD) of three independent experiments. Compared with oxaliplatin, $*p < 0.05$, $**p < 0.01$.

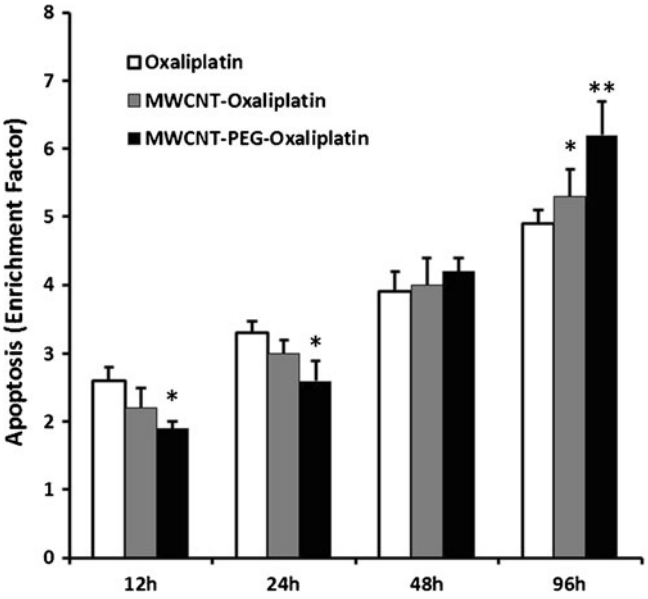

Fig. 10 Effect of oxaliplatin, MWCNT-Oxaliplatin and MWCNT-PEG-Oxaliplatin on the cell apoptosis of HT29 human colon adenocarcinoma. Compared with oxaliplatin, $*p < 0.05$, $**p < 0.01$.

in delivery system, since their high length-to-diameter ratio is advantageous to cargo molecules storage and cellular uptake, and their stable physicochemical property is beneficial to various chemical functionalisation. Here we report the successful encapsulation of oxaliplatin, an FDA-approved anticancer drug, into PEGylated multi-walled carbon nanotubes (MWCNT-PEG). To avoid introducing toxic adjuvant material should be another concern during the development of nanotube formulations. In our investigation, the cytotoxicity of MWCNTs was effectively decreased by functionalisation with PEG, in concomitance with its improved solubility in water. More importantly, the presence of PEG molecules could slow down the release rate of oxaliplatin from cavity of MWCNTs, thus reducing the escape of such hydrophilic molecules prior to reaching tumors. Therefore, MWCNT-PEG-oxaliplatin helped delivery more drug molecules into tumor cells and mitigated its cytotoxicity to normal cells as well. As a result, the cytotoxicity of MWCNT-PEG-oxaliplatin to HT-29 showed a great improvement in comparison to oxaliplatin alone and MWCNT-oxaliplatin.

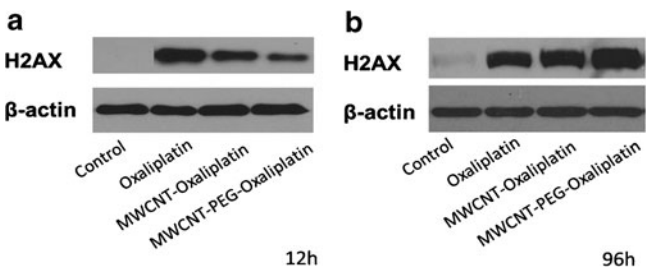

Fig. 9 Representative Western blot analysis of oxaliplatin, MWCNT-Oxaliplatin and MWCNT-PEG-Oxaliplatin induced γ-H2AX formation in HT29 human colon adenocarcinoma cells after a (**a**) 12 and (**b**) 96 h treatment.

CONCLUSIONS

In this manuscript, we have demonstrated that MWCNTs could be used as a promising carrier for drug delivery. Through functionalisation on external surface and encapsulation of oxaliplatin into inner cavity, a great amount of oxaliplatin was loaded into MWCNT-COOH and MWCNT-PEG. And the following release showed that the entrapped oxaliplatin could readily move out of MWCNT-COOH and MWCNT-PEG in aqueous environment. Furthermore, PEGylation of MWCNTs was able to retard the release rate of oxaliplatin, thus remarkably improved the pharmaceutical action of oxaliplatin to HT-29 cells. Therefore, we envision this delivery system could potentially be useful for treatment of cancer. Future work will include the design of targeted delivery of MWCNTs drug carrier by combining MWCNT-PEG with some target agents (i.e. bevacizumab, cetuximab, panitumumab, etc.) with the purpose of improving bioavailability, preventing rapid deactivation and elimination of these antibodies by the body.

REFERENCES

1. Chiu SJ, Chao JI, Lee YJ, Hsu TS. Regulation of gamma-H2AX and securin contribute to apoptosis by oxaliplatin via a p38 mitogen-activated protein kinase-dependent pathway in human colorectal cancer cells. Toxicol Lett. 2008;179(2):63–70. Epub 2008/05/24.
2. Simpson D, Dunn C, Curran M, Goa KL. Oxaliplatin: a review of its use in combination therapy for advanced metastatic colorectal cancer. Drugs. 2003;63(19):2127–56. Epub 2003/09/10.
3. Alcindor T, Beauger N. Oxaliplatin: a review in the era of molecularly targeted therapy. Curr Oncol. 2011;18(1):18–25. Epub 2011/02/19.
4. Mani S, Graham MA, Bregman DB, Ivy P, Chaney SG. Oxaliplatin: a review of evolving concepts. Cancer Invest. 2002;20 (2):246–63. Epub 2002/03/21.
5. James E, Podoltsev N, Salehi E, Curtis BR, Saif MW. Oxaliplatin-induced immune thrombocytopenia: another cumulative dose-dependent side effect? Clin Colorectal Cancer. 2009;8(4):220–4. Epub 2009/10/14.
6. Samol J, Waterston A. Oxaliplatin-induced coronary artery spasm: first report of an important side-effect. BMJ Case Rep. 2009;2009. Epub 2009/01/01.
7. Pasetto LM, D'Andrea MR, Rossi E, Monfardini S. Oxaliplatin-related neurotoxicity: how and why? Crit Rev Oncol Hematol. 2006;59(2):159–68. Epub 2006/06/30.
8. Xu YY, Du YZ, Yuan H, Liu LN, Niu YP, Hu FQ. Improved cytotoxicity and multidrug resistance reversal of chitosan based polymeric micelles encapsulating oxaliplatin. J Drug Target. 2011;19(5):344–53. Epub 2010/09/22.
9. Franzen U, Nguyen TTTN, Vermehren C, Gammelgaard B, Ostergaard J. Characterization of a liposome-based formulation of oxaliplatin using capillary electrophoresis: encapsulation and leakage. J Pharm Biomed Anal. 2011;55(1):16–22.
10. Suzuki R, Takizawa T, Kuwata Y, Mutoh M, Ishiguro N, Utoguchi N, *et al.* Effective anti-tumor activity of oxaliplatin encapsulated in transferrin-PEG-liposome. Int J Pharm. 2008;346(1–2):143–50.
11. Li JQ, Wang SL, Xu F, Liu ZY, Li R. Therapeutic effectiveness of slow-release PLGA-oxaliplatin microsphere on human colorectal tumor-bearing mice. Anticancer Drugs. 2010;21(6):600–8. Epub 2010/06/10.
12. Iijima S. Helical microtubules of graphitic carbon. Nature. 1991;354(6348):56–8.
13. Bhirde AA, Patel V, Gavard J, Zhang G, Sousa AA, Masedunskas A, *et al.* Targeted killing of cancer cells in vivo and in vitro with EGF-directed carbon nanotube-based drug delivery. ACS Nano. 2009;3(2):307–16. Epub 2009/02/25.
14. Serag MF, Kaji N, Gaillard C, Okamoto Y, Terasaka K, Jabasini M, *et al.* Trafficking and subcellular localization of multiwalled carbon nanotubes in plant cells. ACS Nano. 2011;5(1):493–9. Epub 2010/12/15.
15. Hilder TA, Hill JM. Carbon nanotubes as drug delivery nanocapsules. Curr Appl Phys. 2008;8(3–4):258–61.
16. Tasis D, Tagmatarchis N, Bianco A, Prato M. Chemistry of carbon nanotubes. Chem Rev. 2006;106(3):1105–36.
17. Zhao B, Hu H, Yu A, Perea D, Haddon RC. Synthesis and characterization of water soluble single-walled carbon nanotube graft copolymers. J Am Chem Soc. 2005;127(22):8197–203. Epub 2005/06/02.
18. Ajima K, Yudasaka M, Murakami T, Maigne A, Shiba K, Ijima S. Carbon nanohorns as anticancer drug carriers. Mol Pharm. 2005;2(6):475–80.
19. Feazell RP, Nakayama-Ratchford N, Dai H, Lippard SJ. Soluble single-walled carbon nanotubes as longboat delivery systems for Platinum(IV) anticancer drug design. J Am Chem Soc. 2007;129 (27):8438–9.
20. Ren HX, Chen X, Liu JH, Gu N, Huang XJ. Toxicity of single-walled carbon nanotube: how we were wrong? Mater Today. 2010;13(1–2):6–8.
21. Nayak TR, Leow PC, Ee PLR, Arockiadoss T, Ramaprabhu S, Pastorin G. Crucial parameters responsible for carbon nanotubes toxicity. Curr Nanosci. 2010;6(2):141–54.
22. Xu JM, Song ST, Tang ZM, Liu XQ, Jiang ZF, Zhou L, *et al.* Evaluation of in vitro chemosensitivity of antitumor drugs using the MTT assay in fresh human breast cancer. Breast Cancer Res Treat. 1998;49(3):251–9. Epub 1998/10/17.
23. Xu JM, Azzariti A, Colucci G, Paradiso A. The effect of gefitinib (Iressa, ZD1839) in combination with oxaliplatin is schedule-dependent in colon cancer cell lines. Cancer Chemother Pharmacol. 2003;52(6):442–8. Epub 2003/09/19.
24. Walker DL, Reid JM, Svingen PA, Rios R, Covey JM, Alley MC, *et al.* Murine pharmacokinetics of 6-aminonicotinamide (NSC 21206), a novel biochemical modulating agent. Biochem Pharmacol. 1999;58(6):1057–66. Epub 1999/10/06.
25. Balin-Gauthier D, Delord JP, Pillaire MJ, Rochaix P, Hoffman JS, Bugat R, *et al.* Cetuximab potentiates oxaliplatin cytotoxic effect through a defect in NER and DNA replication initiation. Br J Cancer. 2008;98(1):120–8. Epub 2008/01/10.
26. Yudasaka M, Ajima K, Suenaga K, Ichihashi T, Hashimoto A, Iijima S. Nano-extraction and nano-condensation for C-60 incorporation into single-wall carbon nanotubes in liquid phases. Chem Phys Lett. 2003;380(1–2):42–6.
27. Li J, Yap SQ, Yoong SL, Nayak TR, Chandra GW, Ang WH, *et al.* Carbon nanotube bottles for incorporation, release and enhanced cytotoxic effect of cisplatin. Carbon. 2012;50 (4):1625–34.
28. Ajima K, Yudasaka M, Maigne A, Miyawaki J, Iijima S. Effect of functional groups at hole edges on cisplatin release from inside single-wall carbon nanohorns. J Phys Chem B. 2006;110 (11):5773–8.
29. Worle-Knirsch JM, Pulskamp K, Krug HF. Oops they did it again! Carbon nanotubes hoax scientists in viability assays. Nano Lett. 2006;6(6):1261–8. Epub 2006/06/15.
30. Zhang Y, Xu Y, Li Z, Chen T, Lantz SM, Howard PC, *et al.* Mechanistic toxicity evaluation of uncoated and PEGylated single-walled carbon nanotubes in neuronal PC12 cells. ACS Nano. 2011;5(9):7020–33. Epub 2011/08/27.
31. Coccini T, Roda E, Sarigiannis DA, Mustarelli P, Quartarone E, Profumo A, *et al.* Effects of water-soluble functionalized multi-walled carbon nanotubes examined by different cytotoxicity methods in human astrocyte D384 and lung A549 cells. Toxicology. 2010;269(1):41–53. Epub 2010/01/19.
32. Han YG, Xu J, Li ZG, Ren GG, Yang Z. In vitro toxicity of multi-walled carbon nanotubes in C6 rat glioma cells. Neurotoxicology. 2012. Epub 2012/06/26.
33. Chaney SG, Campbell SL, Bassett E, Wu Y. Recognition and processing of cisplatin- and oxaliplatin-DNA adducts. Crit Rev Oncol Hematol. 2005;53(1):3–11. Epub 2004/12/21.
34. Jamieson ER, Lippard SJ. Structure, recognition, and processing of cisplatin-DNA adducts. Chem Rev. 1999;99(9):2467–98. Epub 2001/12/26.
35. Johnson SW, Perez RP, Godwin AK, Yeung AT, Handel LM, Ozols RF, *et al.* Role of platinum-DNA adduct formation and removal in cisplatin resistance in human ovarian cancer cell lines. Biochem Pharmacol. 1994;47(4):689–97. Epub 1994/02/11.
36. Cadet J, Bellon S, Douki T, Frelon S, Gasparutto D, Muller E, *et al.* Radiation-induced DNA damage: formation, measurement, and biochemical features. J Environ Pathol Toxicol Oncol: official organ of the International Society for

Environmental Toxicology and Cancer. 2004;23(1):33–43. Epub 2004/03/05.
37. Asaithamby A, Chen DJ. Cellular responses to DNA double-strand breaks after low-dose gamma-irradiation. Nucleic Acids Res. 2009;37(12):3912–23. Epub 2009/04/30.
38. Taneja N, Davis M, Choy JS, Beckett MA, Singh R, Kron SJ, *et al.* Histone H2AX phosphorylation as a predictor of radiosensitivity and target for radiotherapy. J Biol Chem. 2004;279(3):2273–80. Epub 2003/10/17.
39. Celeste A, Fernandez-Capetillo O, Kruhlak MJ, Pilch DR, Staudt DW, Lee A, *et al.* Histone H2AX phosphorylation is dispensable for the initial recognition of DNA breaks. Nat Cell Biol. 2003;5(7):675–9. Epub 2003/06/07.
40. Furuta T, Takemura H, Liao ZY, Aune GJ, Redon C, Sedelnikova OA, *et al.* Phosphorylation of histone H2AX and activation of Mre11, Rad50, and Nbs1 in response to replication-dependent DNA double-strand breaks induced by mammalian DNA topoisomerase I cleavage complexes. J Biol Chem. 2003;278(22):20303–12. Epub 2003/03/28.